Simultaneous Synchrotron Radiation X-ray Diffraction–DSC Analysis of Melting and Crystallization Behavior of Trilauroylglycerol in Nanoparticles of Oil-in-Water Emulsion

M. Higami[a], S. Ueno[a], T. Segawa[b], K. Iwanami[b], and K. Sato[a,*]

[a]Biomolecular Physical Chemistry Group, Graduate School of Biosphere Science, Hiroshima University, Higashi-Hiroshima, 739-8528, Japan, and [b]Food Research Laboratory, Nippon Oil & Fats Co., Tokyo, 114-0003, Japan

ABSTRACT: Crystallization, polymorphic transformation, and melting behavior of nanoparticles of trilauroylglycerol (LLL) in oil-in-water (O/W) emulsion were examined initially by DSC, and then by simultaneous synchrotron radiation small-angle (SAXS) and wide-angle (WAXS) X-ray diffraction and DSC (SR-SAXS/WAXS/DSC). The O/W nanoparticles emulsions having average diameters of 42 to 120 nm were prepared by application of mechanical shear using a high-pressure homogenizer. The following results were obtained: (i) The DSC study showed that the melting temperature of the stable β form of LLL was reduced from 46.7 (bulk) to 26.5–44.0°C (nanoparticles); this variation was assumed to be due to the size distribution of the nanoparticles. Crystallization temperature was also reduced from 18.9 (bulk) to –9.5 ± 0.5°C (nanoparticles). These results were consistent with those of previous studies of nanoparticles of fats obtained in the O/W emulsion. (ii) The results obtained by the SR-SAXS/WAXS/DSC technique during the cooling process to –20°C showed that the first-occurring polymorph of LLL in the bulk liquid was β′, whereas α was first nucleated and transformed to β′ around –10°C during cooling in the nanoparticles. (iii) The SR-SAXS/WAXS/DSC data taken during the heating process from –20°C after the crystallization showed that β′ transformed to β around 0°C and that the melting of β started at 30°C and ended at 44°C. The present study showed that forming nanoparticles of LLL in the O/W emulsion having the diameters of 42 to 120 nm reduced the melting and crystallization temperatures and increased the transformation rate of $\alpha \rightarrow \beta' \rightarrow \beta$ in comparison to the LLL crystals formed in the bulk phase.

Paper no. J10351 in *JAOCS 80*, 731–739 (August 2003).

KEY WORDS: Nanoparticles, O/W emulsion, polymorphism, trilauroylglycerol.

Formation of particles of fats and oils in a water phase [oil-in-water (O/W) emulsion] with diameters less than about 200 nm (hereafter referred to as a nanoemulsion) has recently been investigated with a particular emphasis of application to pharmaceuticals (1–3). A nanoemulsion in general exhibits many advantages, such as emulsion stability, transparency, permeability, and easy handling for production processes. The O/W nanoemulsion involving fat crystals within the particles also exhibits desirable properties, such as controlled release of functional lipophilic materials that are incorporated in the fat particles (4–11). Physical properties of melting, crystallization, and polymorphic transformation of fats in the nanoemulsion have been studied by multiple techniques (12–16). In particular, X-ray diffraction studies using synchrotron radiation (SR-XRD) have been performed by Westesen and coworkers (12,17–22) to observe structural and thermal properties of crystalline nanoparticles of TAG. In their work, data from SR-XRD and DSC, although the two methods were employed in a separate way, were discussed in terms of crystallization, polymorphic transformation, and melting behavior as a function of varying size of the nanoemulsion particles. In particular, the precise correlation of linewidth of small-angle SR-XRD spectra with the DSC thermopeaks indicated that the reduction in melting temperature of TAG crystals was related to the reduction in particle size and that the number of TAG lamellae in a crystal was also reduced to 2–3 when the particle diameter was reduced to 10–100 nm (18–22).

The present paper reports experimental results of SR-XRD and DSC experiments that were performed simultaneously for the same nanoemulsion particles of trilauroylglycerol (LLL). As for the SR-XRD measurement, small-angle (SAXS) and wide-angle (WAXS) X-ray scattering were monitored at the same time (SR-SAXS/WAXS/DSC experiments). In this study, a temperature-controlled DSC pan containing nanoemulsion particles was exposed to an SR-X-ray beam so that the SR-XRD and DSC measurements were performed at the same time. Such a simultaneous measurement has recently revealed microscopic and dynamic features of crystallization and polymorphic transformation of fats in bulk (23–26) and emulsion particles (27–29).

In the present study, LLL was chosen as a model substance mainly because LLL represents a typical saturated-acid TAG whose physical properties are commonly observed in the other fats. The other reasons are that the important properties of crystallization and polymorphic transformation of LLL in bulk and emulsion (19,30) states are well known; thus, the present work can be compared to past work.

*To whom correspondence should be addressed at Biomolecular Physical Chemistry Group, Graduate School of Biosphere Science, Hiroshima University, 1-4-4 Kagamiyama, Higashi-Hiroshima, 739-8528, Japan.

E-mail: kyosato@hiroshima-u.ac.jp

The results obtained in the present study were basically consistent with those of a recent study of the nanoemulsion LLL particles with respect to melting (20). However, clear correspondences between the occurrence of and variation in lamellar stacking (SAXS) and subcell packing (WAXS) data to DSC peaks could shed light on the crystallization, polymorphic transformation, and melting of three polymorphs, α, β′ and β, of LLL crystals in the nanoemulsion particles.

MATERIALS AND METHODS

The nanoparticles of LLL in the O/W emulsion were prepared by using LLL purchased from Sigma Chemicals (St. Louis, MO), polyglycerol FA esters (Sakamoto Pharmaceuticals, Osaka, Japan), and distilled water.

Nanoemulsion particles were prepared as follows. Large-sized O/W emulsions (diameters > several μm) were prepared with a homomixer (4000 rpm, 5 min) by using LLL, polyglycerine FA esters (stearic and lauric acid moieties) as emulsifying agents, and distilled water at 60°C. The mixture was poured into a high-pressure homogenizer (Microfluidizer M110-E/H; Mizuho Industrial Co., Osaka, Japan) at 60°C, and a pressure of 80, 110, and 150 MPa was applied to obtain the O/W nanoemulsion particles. To observe the effects of variations in the concentration of fat and emulsifiers on the nanoemulsion properties, two concentrations of LLL (10 and 20 wt%) and two concentrations of emulsifiers (20 and 40 wt% with respect to the total weight of emulsion) were examined. Particle size distribution was analyzed with a submicron particle analyzer (Coulter model N4 SD; Beckman-Coulter) at 20°C.

Table 1 shows the size distribution of the nanoemulsion particles prepared under three combinations of oil–emulsifier–water concentrations (wt%), 10:20:70, 20:20:60, and 20:40:40, with different homogenization pressure and frequency (number of passes) of homogenization. It appears that a systematic relationship between the size distribution and homogenization conditions does not exist. For example, a single-peak size distribution was observed for samples A, E, F, and I, whereas a double-peak size distribution was observed for B, C, D, G, and H. However, some tendency was detectable in that the average size of the nanoemulsion particles was reduced as the pressure of homogenizer was increased and as the frequency (number of passes) of homogenization with the same pressure increased. For example, sample A (average diameter 42 nm) was formed by passing through the homogenizer three times at a pressure of 150 MPa, whereas larger droplets were formed by passing once at the same pressure (Samples C, G, and I). Another tendency was that the droplet sizes were reduced by increasing the concentrations of emulsifiers when prepared under the same homogenization conditions, as shown in samples G and I.

DSC measurements were done by using a Rigaku Thermoplus DSC 8240 instrument (Tokyo, Japan). The methods of the SR-SAXS/WAXS/DSC experiments were fully described elsewhere (23,24). Briefly, the SR-SAXS/WAXS/DSC experiments were carried out at a beam line BL-15A of the source "Photon Factory," which was operated at 2.5 GeV at the National Laboratory for High Energy Physics (Tsukuba, Japan). The double-focusing camera was operating at a wavelength of 0.15 nm for the SR-SAXS/WAXS. Temperature during the SR-XRD-DSC simultaneous measurements was varied in the following way: The nanoemulsion-containing sample was heated to 70°C and held at that temperature for 15 min, cooled to –30°C at a rate of 2°C/min, held at –30°C for 5 min, and then heated to 50°C at a rate of 2°C/min. Maximum temperatures, if special reference is not given, defined the temperatures of the DSC endothermic and exothermic peaks.

RESULTS

Figure 1 shows the DSC cooling and heating thermopeaks of the bulk sample. An exothermic peak appeared at 16.3°C during cooling, whereas an exothermic peak at 23.5°C and an endothermic peak at 46.7°C were observed during heating. As shown below in the SR-SAXS/WAXS/DSC data, the β′ form crystallized at 16.3°C and transformed to β at 23.5°C, then β melted at 46.7°C.

Figure 2 shows the DSC cooling and heating thermopeaks of nanoemulsions A through E that were observed at the ratio of O/W = 10:70 and emulsifier concentration of 20 wt%. The average size of the five samples varied from 42 (sample A) to

TABLE 1
Preparation and Particle-Size Parameters of the Nanoemulsion Particles

Sample	Content of oil (%)	Amount of emulsifier (%)	Average particle diameter (nm)	Homogenization condition	
				Pressure (MPa)	Frequency (no. of passes)
A	10	20	42	150	3
B	10	20	49	110	3
C	10	20	80	150	1
D	10	20	95	110	1
E	10	20	120	80	1
F	20	20	60	150	3
G	20	20	98	150	1
H	20	40	50	150	2
I	20	40	66	150	1

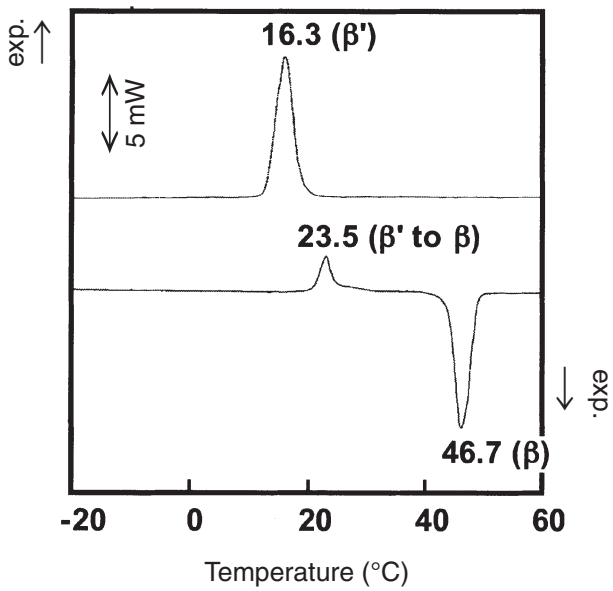

FIG. 1. The DSC cooling and heating thermopeaks of the bulk samples.

120 nm (sample E). A single exothermic peak appeared at –9.5 ± 0.5°C when the five samples were cooled. The onset temperatures were –7.5 ± 0.5°C. These values are well below those of LLL in bulk (16.3°C, Fig. 1) and emulsion particles having diameters of 360 nm (1.0°C), which were determined by ultrasound velocity measurement (30). Crystallization temperature did not decrease when the average size of the nanoemulsion droplets decreased from 120 to 42 nm. However, Bunjes *et al.* (19) reported that crystallization temperatures of trimyristoylglycerol (MMM) and tripalmitoylglycerol (PPP) nanoparticles were decreased by less than 2°C with decreasing particle sizes.

In contrast, the heating DSC thermopeaks of the nanoemulsions exhibited multiple endothermic peaks in a temperature range of 27 to 40°C, and these peaks corresponded to melting of LLL crystals in the droplets (see below). The relative sizes of the melting peaks in Figure 2 are summarized in Table 2. The m.p. of the five nanoemulsions were lower than that of the bulk LLL, and the peak sizes of high-temperature peaks (around 38°C) became larger than those of low-temperature peaks (around 27°C) as the average size of the nanoemulsion increased.

According to Westesen *et al.* (17–21), reduction in the melting temperature of the TAG crystals in the nanoemulsions is caused by a size effect of the crystal particle in which the reduced nanoemulsion diameter (D) may cause the reduction of the melting temperature of β of LLL from 46.7°C (bulk) to ~40°C (D ~ 20 nm) and 36°C (D ~ 10 nm). Since there is a size distribution in the nanoemulsions, large-sized particles exhibited high melting temperatures and vice versa, thus resulting in multiple DSC melting profiles (18,19). In the present case, the same interpretation can be applied.

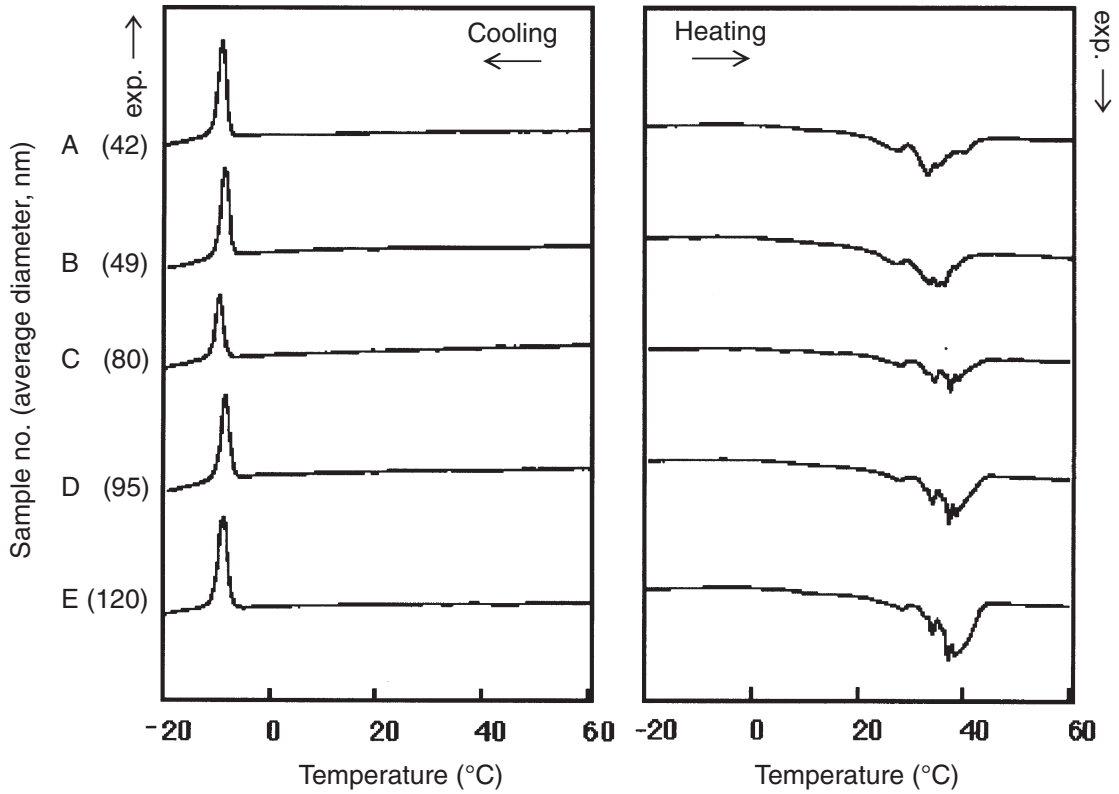

FIG. 2. The DSC cooling and heating thermopeaks of the nanoemulsions. Five samples were made with an oil/water ratio of 10:90 and with an emulsifier concentration of 20 wt%.

TABLE 2
DSC Endothermic Peaks (°C) Nanoemulsions[a]

Sample	Oil/water = 10:90	Sample	Oil/water = 20:80
A	27.6 (M), 33.2 (L), 34.8 (M), 39.8 (S)	F	35.2 (S), 37.4 (S), 39.0 (L), 39.9 (L), 44.0 (S)
B	27.8 (M), 33.5 (L), 35.2 (L), 36.5 (L), 38.5 (S)	G	34.3 (S), 37.0 (M), 38.7 (L), 39.9 (L)
C	27.7 (M), 34.2 (L), 37.3 (L), 38.7 (S)	H	28.5 (M), 35.0 (L), 37.5 (M), 41.3 (S)
D	27.9 (S), 34.3 (M), 37.4 (L), 38.8 (M)	I	26.5 (S), 29.7 (M), 33.9 (M), 35.2 (L), 37.7 (L)
E	28.2 (S), 34.1 (M), 37.2 (L), 38.2 (L)		

[a]L, large; M, medium; S, small.

Figure 3 shows the DSC thermopeaks during cooling and heating of four samples made of oil/water = 20:60 with the emulsifier concentrations of 20 and 40 wt%. The average size of the droplets was reduced when the emulsifier concentration was increased, because small-size droplets were easily formed with higher concentrations of emulsifiers. Like the results shown in Figure 2, a single exothermic and multiple endothermic peaks were observed for each sample during cooling and heating process, respectively. Although the single exothermic peak during cooling did not vary among four samples, the range of temperature where the endothermic peaks appeared during heating was different between the two sample groups formed with the emulsifier concentrations of 20 wt% (F and G) and 40 wt% (H and I), as shown in Figure 3 and Table 2. This result also indicates that the sizes of the droplets became smaller for the samples H and I than for the samples F and G, and the melting temperature of LLL in the small-sized droplets was reduced.

Figure 4 shows the simultaneous SR-SAXS/WAXS/DSC measurements of the bulk LLL samples. In Figure 4A, crystallization of β′ of LLL is shown, as reflected by the SAXS peaks at 3.46 nm, two WAXS peaks at 0.425 and 0.388 nm, and a DSC exothermic peak at 17.9°C. The difference in the crystallization temperatures between the results in Figure 2 (16.3°C) and Figure 4 (17.9°C) may be due to differences in the DSC apparatus employed. Figure 4B, made during heating of the sample after cooling (shown in Fig. 4A) shows that β′ transformed to β at 22.8°C, as exhibited by changes of the

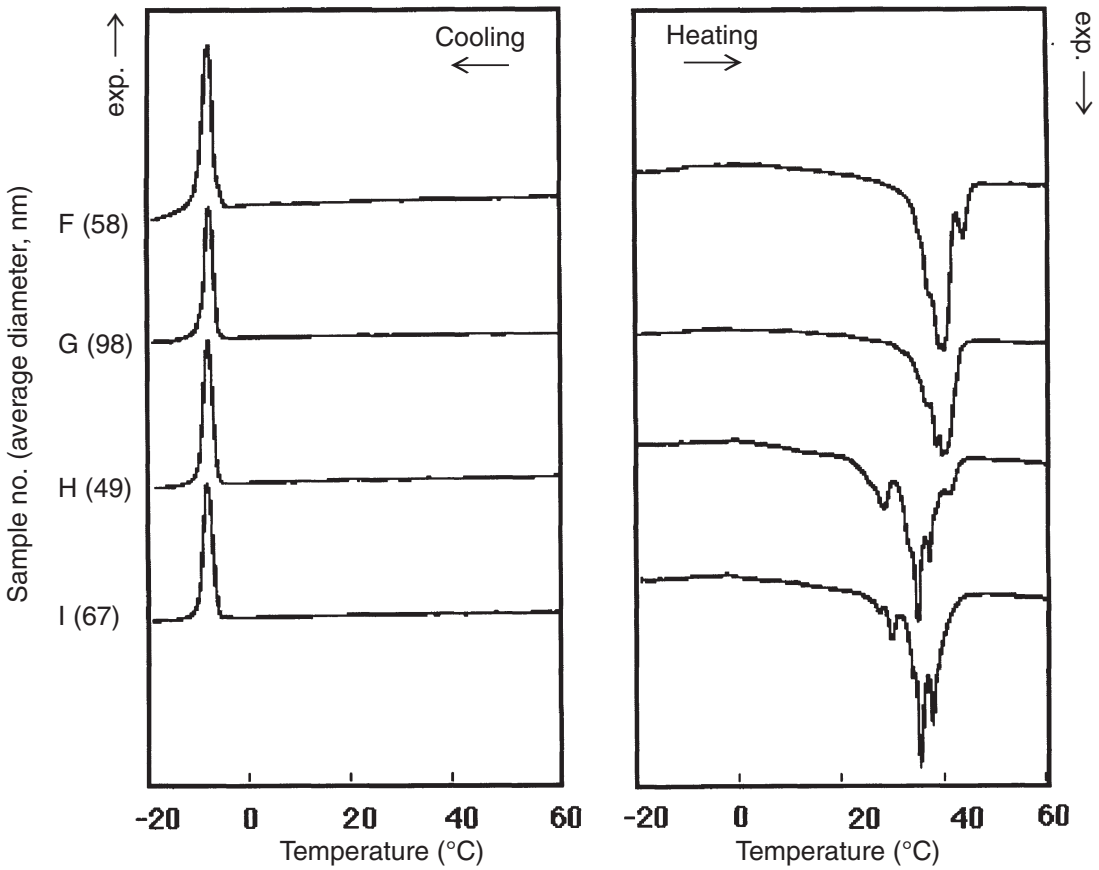

FIG. 3. The DSC thermopeaks of nanoemulsions made with an oil/water ratio of 20:80 and emulsifier concentrations of 20 and 40 wt%.

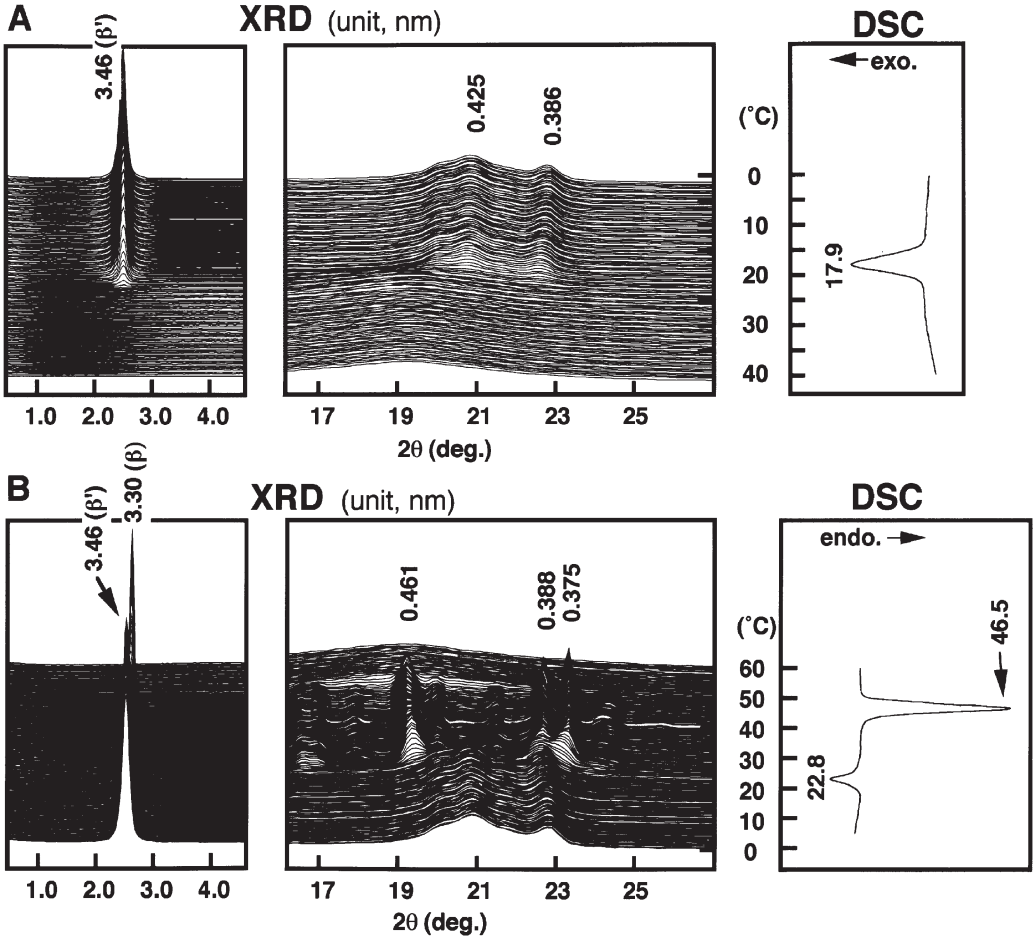

FIG. 4. Simultaneous small-angle X-ray scattering (SAXS)/wide-angle X-ray scattering (WAXS) synchrotron radiation (SR)-X-ray diffraction (XRD) and DSC measurements of the bulk trilauroylglycerol (LLL) samples.

SAXS peaks from 3.46 (β′) to 3.30 nm (β), and in changes of the WAXS peaks from double (β′) to multiple peaks (β). On further heating, β crystals melted at 46.5°C, as shown by the disappearance of the SAXS and WAXS peaks and by the occurrence of a large DSC endothermic peak.

Figures 5A and 5B show the SR-SAXS/WAXS/DSC data of nanoemulsion sample G (see Table 1), having an average diameter of 98 nm, during cooling and heating, respectively. In Figure 5A, a DSC exothermic peak and a corresponding single WAXS peak (0.398 nm) appeared at –8.5°C, both indicating the crystallization of the α form of LLL. During further cooling to –20°C, the SAXS and WAXS peaks converted to 3.46 and 0.425 nm around –10°C, respectively. This change corresponded to the transformation from α to β′, although this was not detectable by DSC. Figure 5B shows that the SAXS and WAXS peaks of β′ gradually converted to those of β around 0°C during heating, although a broad exothermic peak was detected by DSC. On further heating, multiple DSC endothermic peaks appeared in a temperature range of 37 to 41°C. This range of melting temperature was in good agreement with that shown in Figure 3. The SR-SAXS/WAXS spectra of β were maintained up to about 44°C, where all SR-XRD spectra disappeared by melting.

From the result shown in Figure 5, it can be concluded that (i) LLL in the nanoemulsion particles having an average diameter of 98 nm crystallized in α, (ii) that the α crystals transformed to β′ during cooling, (iii) that, during heating, β′ of LLL transformed to β around 0°C, and finally (iv) that β of LLL melted at around 37 to 41°C. This feature was quite different from that observed for the bulk state of LLL, since α does not crystallize on cooling at a rate of 2°C/min, and β′ also does not transform to β around 0°C in the bulk crystal. In the bulk state, β′ transformed to β at around 22–23°C as shown in Figures 1 and 4. Although not shown here, we confirmed that the α form of LLL, which was crystallized by rapid cooling from bulk liquid, did not transform to β′ below 0°C over a few days.

Figure 6 shows the temperature dependence of the intensity of the SAXS peaks of β of LLL in the bulk and the nanoemulsion (sample G). The intensity of every SAXS peak was calculated from the total area of the diffraction spectrum at each temperature. With the bulk sample (Fig. 6A), the spectral intensity started to decrease around 41°C and rapidly decreased around 45°C and disappeared at 49°C. This behavior is quite consistent with that of the DSC melting thermopeaks shown in Figures 1 and 4. As for the nanoemulsion sample G

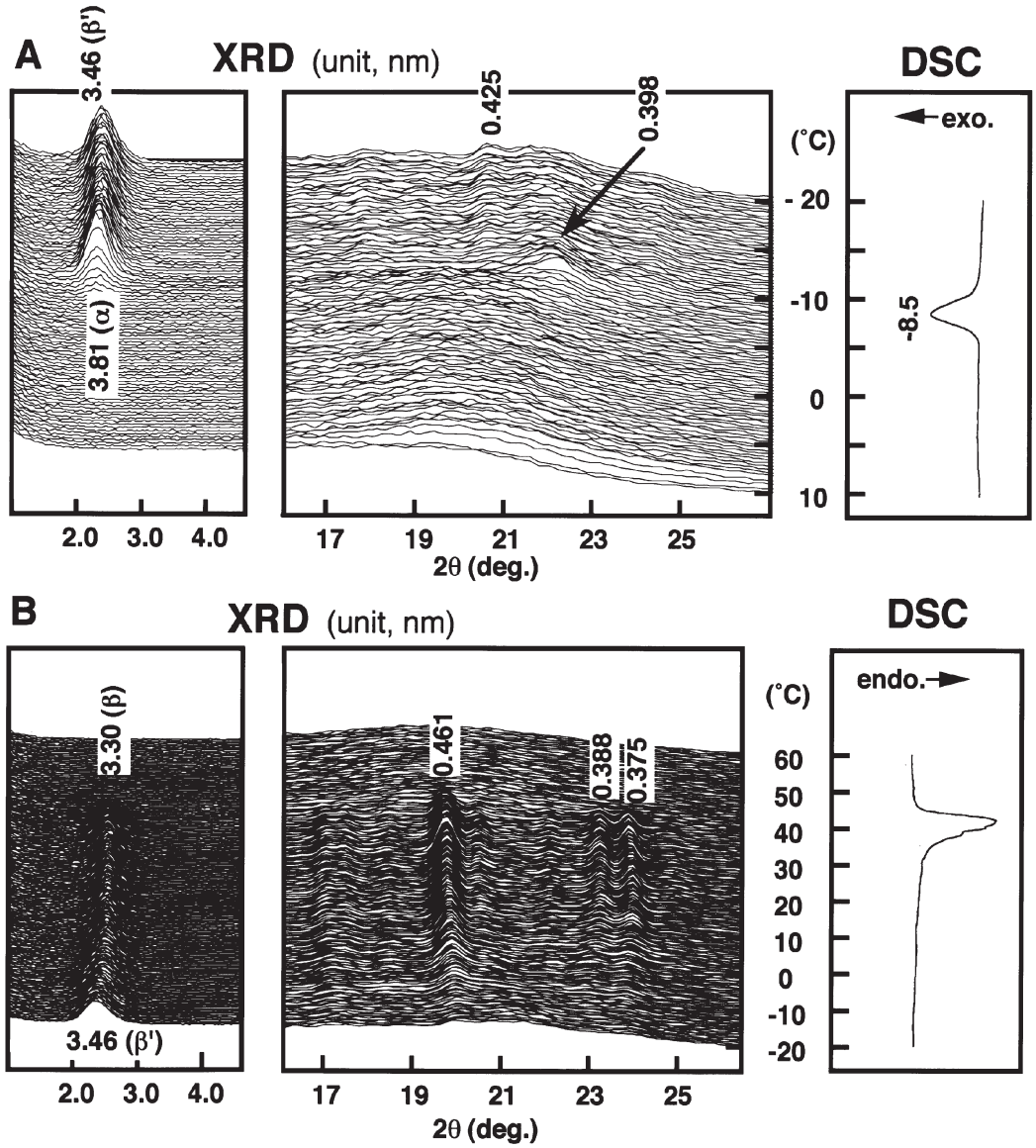

FIG. 5. Simultaneous SAXS/WAXS SR-XRD and DSC measurements of the nanoemulsion (sample G). (A) Cooling, and (B) heating. (A rise in WAXS spectra near 2θ = 15° is not due to diffraction.) For abbreviations see Figure 4.

(Fig. 6B), reduction in diffraction intensity was initiated around 31°C, a gradual decrease was exhibited at 38–41°C, then the spectra disappeared at 42°C, as shown by arrows. This feature of the spectra intensity variation with temperature also showed a good correspondence with the DSC exothermic peaks shown in Figure 5B, indicating multiple melting behavior of LLL crystals in the nanoemulsion droplets. It is reasonable to consider that this multiplicity in the melting peaks is caused by differences in particle sizes of the nanoemulsion: The smaller the sizes, the lower the melting peaks.

DISCUSSION

Characteristics of nanoemulsion particles (average diameter 40–120 nm). (i) Crystallization. Crystallization of nonemulsion particles was retarded compared to the bulk sample. This is due to a size effect, since LLL in the O/W emulsion having an average diameter of 360 nm crystallized at 1.0°C (30). The other lipids in the emulsion droplets showed the same behavior (12).

(ii) Melting temperatures. Melting temperatures of the β forms of LLL were reduced, and multiple melting profiles were observed in the nanoemulsion. The two properties may be due to a decrease in the crystal size itself and to the crystal size distribution.

(iii) Polymorphic crystallization. Polymorphic crystallization behavior was affected by nanoparticle formation, since β′ was crystallized by cooling of bulk liquid at a rate of 2°C, whereas α was crystallized in the nanoemulsion droplets at the same cooling rate.

(iv) Polymorphic transformation. The polymorphic transformation from α to β′ and from β′ to β occurred at –10°C on

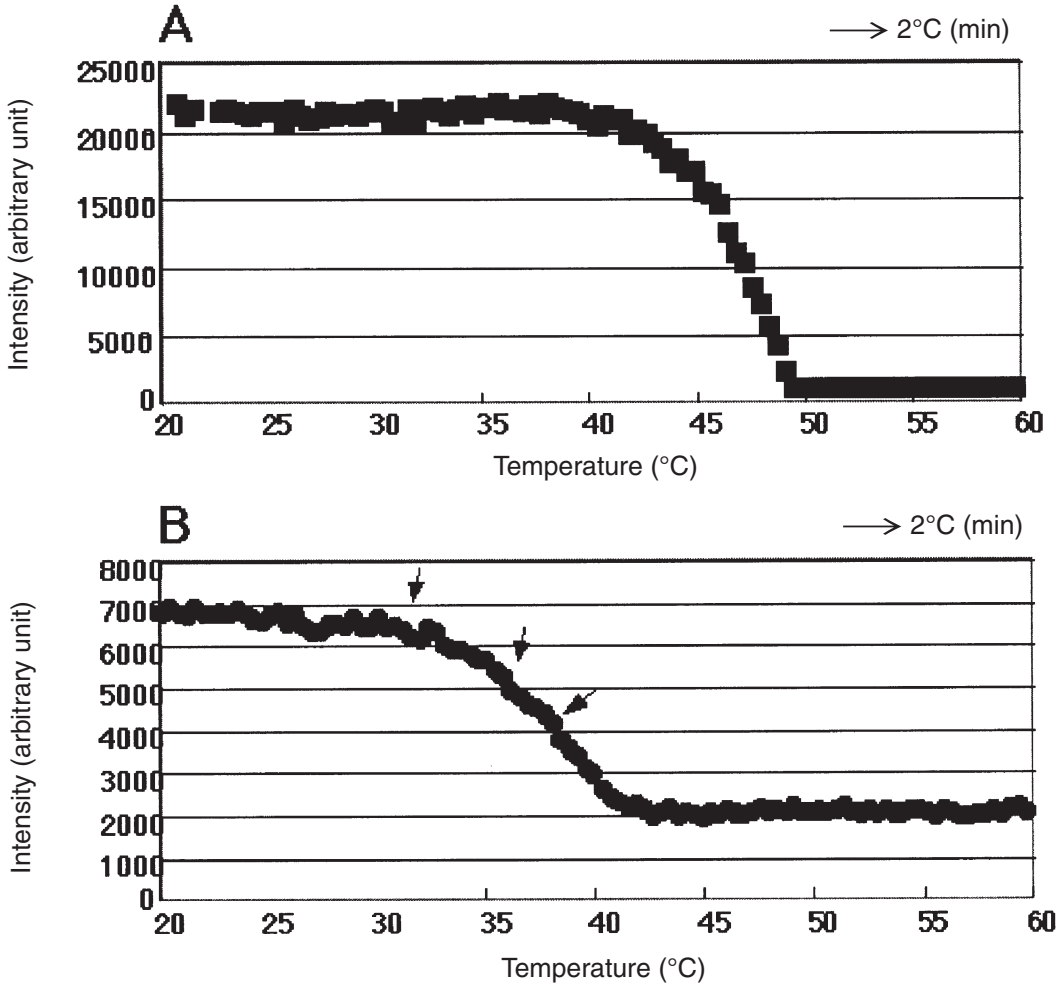

FIG. 6. Temperature dependence of the intensity of SAXS peak diffraction of β of LLL in the bulk (A) and nanoemulsion (B) (sample G). For abbreviations see Figure 4.

cooling, and at 0°C on heating, respectively, in the nanoemulsion. This result was not observed in a previous study (20) in which DSC and SR-XRD were not carried out simultaneously. It was interesting that α transformed to β′ during the cooling process around –10°C. Such a behavior was never observed in the bulk state. Transformations from the least stable α form to the more stable β′ or β forms usually occur in the bulk state during heating by the absorption of the thermal energy that is necessary to overcome activation energy for the transformation. This means that the $\alpha \rightarrow \beta'$ transformation of LLL crystals in the nanoemulsion during the cooling process was observed for the first time in the present study.

The results regarding crystallization and melting temperatures (points i and ii above) are essentially the same as those of Westesen's group (18–20), although the particles employed in the present study (40–120 nm) were a bit smaller than theirs (100–200 nm). The results regarding polymorphic crystallization and transformation (points iii and iv above) were observed (*in situ*) for the first time in this study. That is, the stable β form was easily formed through the polymorphic transformation from the initially crystallized α form to the metastable β′ form, and by successive transformation from β′ to β; both transformations occurred during the cooling and heating process below 0°C.

Characteristics of fat crystallization in emulsion droplets. (i) Reduced rate of nucleation of crystals. This reduced rate is reflected in the increase of supercooling for crystallization. This was observed in the present study using the nanometer-sized emulsion particles, and also in the μm-size particles reported in other work (19).

The reduced rate of nucleation of crystals in the emulsion droplets may be explained by two effects: redistribution of nucleation-catalyzing impurity substances into the particles, in which diluted impurity molecules do not promote heterogeneous nucleation of crystals (31); and the decreased number of molecules of crystallizing substance present in the emulsion particles reduced the rate of transformation from molecular clusters to crystal nuclei. In an extreme case of redistribution of impurities, where few catalytic impurities are activated in the interior volume of the particles and at the oil–water interface, the nature of the nucleation process may change from heterogeneous to homogeneous, provided that

the interactions between the emulsifier molecules and LLL molecules do not affect the nucleation process. It is quite difficult to assess which cause is primarily operating in the crystallization processes examined in the present study.

(ii) Complicated nucleation processes. Complicated nucleation processes are caused by the presence of oil–water interfaces constructed by emulsifier membranes. In particular, heterogeneous nucleation catalyzed at the interface (surface heterogeneous nucleation) is a new phenomenon that is less significant for the nucleation in the bulk state. Furthermore, the importance of surface heterogeneous nucleation may be increased with decreasing particle diameter, because of relative importance of the interface compared to the interior oil phase. It is rather difficult to assess which type of surface heterogeneous nucleation occurred in the nanoemulsion particles examined in the present study. To examine this, one may have to vary the surface structures of the O/W emulsion, either by changing the emulsifiers or by using surface-activating additives. In the O/W emulsion particles having μm-sized diameter, surface heterogeneous nucleation was activated by the emulsifier additives (32–34).

(iii) Catalysis of crystallization. Crystallization can be catalyzed by particle–particle interactions resulting from particle collisions (31). Supercooled oil particles are readily crystallized through collision with droplets whose oil phases are already crystallized. It is expected that the crystallization of this type may be enhanced in polydispersed particles rather than in monodispersed particles. Since the particle size distributions obtained in the present study are of polydispersed type, particle–particle interactions may be occurring.

As for the reduction in the crystallization temperature and the enhanced transformation from α to β′ and from β′ to β, both properties are ascribed to physical and structural properties of nanosized particles of fat crystals.

Two main causes may be considered. The first is surface effects, in which excess surface free energy raises the total Gibbs free energy that causes a decrease in m.p. and an increase in solubility (Gibbs–Thomson effect) (35). The surface effect also may be reflected in polymorphic transformations, which are associated with conversions in subcell structures and interlamellar distances, since the polymorphic transformation may be initiated from the crystal surface as a kind of planar defect. Second, the polymorphic transformations also may be initiated from lattice defects, e.g., dislocation or stacking faults, which may be introduced more easily in the nanometer-sized particles compared with the bulk crystals.

The interlamellar distances of LLL crystals in the nanoemulsion particles used in our study are 3.3 (β), 3.5 nm (β′), and 3.8 nm (α). Hence, a particle having a diameter of 40 nm, for example, may contain LLL crystals consisting of about 9 lamellae, if the thickness of the emulsifier molecule (about 4 nm) is subtracted. In the work done by Bunjes' group (18), the number of lamellae planes of trimyristoylglycerol (MMM) crystals in nanoemulsion droplets was estimated by analyzing small-angle XRD spectra. The estimated number of MMM lamellae in the particles having an m.p. around 40°C (*cf.* m.p. in the bulk state, 57°C) was 2–3. In these tiny particles, it is reasonable to assume that the surface effects discussed above are operating in the melting and transformation processes.

In regard to the polymorphic transformation, fat technologists usually intend to maintain the metastable β′ form by prohibiting the β′ → β transformation, since the β′ → β transformation gives rise to robust effects on the physical properties of end products involving fat crystals, as usually exhibited in food (36) and pharmaceutical applications (7,11). Therefore, if one tries to maintain the β′ form in the nanoemulsion particles, specific steps may be necessary to prohibit the β′ → β transformation, such as using β′-stabilized fat materials, polymorph-controlling emulsifiers, and fat–fat interaction.

ACKNOWLEDGMENTS

This work was supported by Nano-technology project, Ministry of Agriculture, Forestry and Fisheries, Japan. The authors also express deep appreciation to Prof. Yoshiyuki Amemiya and Dr. Yoshinobu Nozue of the University of Tokyo for cooperating in the preparation of the beam line BL-15A at the Photon Factory.

REFERENCES

1. Washington, C., and K. Evans, Release Rate Measurement of Model Hydrophobic Solutes from Submicron Triglyceride Emulsions, *J. Controlled Release 33*:383–390 (1995).
2. Norden, T.P., B. Siekmann, S. Lundquist, and M. Malmsten, Physicochemical Characterisation of a Drug-Containing Phospholipid-Stabilised O/W Emulsion for Intravenous Administration, *Eur. J. Pharm. Sci. 13*:393–401 (2001).
3. Bunjes, H., B. Siekmann, and K. Westesen, Emulsions of Supercooled Melts—A Novel Drug Delivery System, *Submicron Emulsions in Drug Targeting and Delivery*, edited by S. Benita, Harwood Academic Publishers, Singapore, 1998, pp. 175–204.
4. Vringer, T., and H.A.G. de Ronde, Preparation and Structure of a Water-in-Oil Cream Containing Lipid Nanoparticles, *J. Pharm. Sci. 84*:466–472 (1995).
5. Siekmann, B., and K. Westesen, Investigations on Solid Lipid Nanoparticles Prepared by Precipitation in O/W Emulsions, *Eur. J. Pharm. Biopharm. 43*:104–109 (1996).
6. Freitas, C., and R.H. Muller, Correlation Between Long-term Stability of Solid Lipid Nanoparticles (SLN^{TM}) and Crystallinity of the Lipid Phase, *Ibid. 47*:125–132 (1999).
7. Dingler, H., R.P. Blum, H. Niehus, R.H. Muller, and S. Gohla, Solid Lipid Nanoparticles (SLN^{TM}/LipopearlsTM)—A Pharmaceutical and Cosmetic Carrier for the Application of Vitamin E in Dermal Products, *J. Microencapsul. 16*:751–767 (1999).
8. Jenning, V., M. Schäfer-Korting, and S. Gohla, Vitamin A-Loaded Solid Lipid Nanoparticles for Topical Use: Drug Release Properties, *J. Controlled Release 66*:115–126 (2000).
9. Muller, R.H., K. Mader, and S. Gohla, Solid Lipid Nanoparticles (SLN) for Controlled Drug Delivery—A Review of the State of the Art, *Eur. J. Pharm. Biopharm. 50*:161–177 (2000).
10. Jenning, V., A.F. Thunemann, and S.H. Gohla, Characterisation of a Novel Solid Lipid Nanoparticle Carrier System Based on Binary Mixtures of Liquid and Solid Lipids, *Int. J. Pharm. 199*: 167–177 (2000).
11. Mehnert, W., and K. Mader, Solid Lipid Nanoparticles Production, Characterization and Applications, *Adv. Drug Deliv. Rev. 47*:165–196 (2001).
12. Bunjes, H., K. Westesen, and M.H.J. Koch, Crystallization Tendency and Polymorphic Transitions in Triglyceride Nanoparticles, *Int. J. Pharm. 129*:159–173 (1996).

13. Siekmann, B., and K. Westesen, Thermoanalysis of the Recrystallization Process of Melt-Homogenized Glyceride Nanoparticles, *Colloid. Surf. B 3*:159–175 (1994).
14. Westesen, K., and B. Siekmann, Investigation of the Gel Formation of Phospholipid-Stabilized Solid Lipid Nanoparticles, *Int. J. Pharm. 151*:35–45 (1997).
15. Freitas, C., and R.H. Muller, Effect of Light and Temperature on Zeta Potential and Physical Stability in Solid Lipid Nanoparticle (SLN^{TM}) Dispersions, *Ibid. 168*:221–229 (1998).
16. Jenning, V., K. Mäder, and S.H. Gohla, Solid Lipid Nanoparticles (SLN^{TM}) Based on Binary Mixtures of Liquid and Solid Lipids: A ^{1}H-NMR Study, *Ibid. 205*:15–21 (2000).
17. Westesen, K., B. Siekmann, and M.H.J. Koch, Investigations on the Physical State of Lipid Nanoparticles by Synchrotron Radiation X-ray Diffraction, *Ibid. 93*:189–199 (1993).
18. Unruh, T., H. Bunjes, K. Westesen, and M.H.J. Koch, Observation of Size-Dependent Melting in Lipid Nanoparticles, *J. Phys. Chem. B 103*:10373–10377 (1999).
19. Bunjes, H., M.H.J. Koch, and K. Westesen, Effect of Particle Size on Colloidal Solid Triglycerides, *Langmuir 16*:5234–5241 (2000).
20. Unruh, T., H. Bunjes, K. Westesen, and M.H.J. Koch, Investigations on the Melting Behavior of Triacylglyceride Nanoparticles, *Colloid Polym. Sci. 279*:398–403 (2001).
21. Bunjes, H., and K. Westesen, Influences of Colloidal State on Physical Properties of Solid Fats, in *Crystallization Processes in Fats and Lipid Systems*, edited by N. Garti and K. Sato, Marcel Dekker, New York, 2001, pp. 457–483.
22. Unruh, T., K. Westesen, P. Boecke, P. Lindner, and M.H.J. Koch, Self-Assembly of Triglyceride Nanoparticles in Suspension, *Langmuir 18*:1796–1800 (2002).
23. Minato, A., S. Ueno, K. Smith, Y. Amemiya, and K. Sato, Thermodynamic and Kinetic Study on Phase Behavior of Binary Mixtures of POP and PPO Forming Molecular Compound Systems, *J. Phys. Chem. 101*:3498–3505 (1997).
24. Takeuchi, M., S. Ueno, J. Yano, E. Floter, and K. Sato, Polymorphic Transformation of 1,3-Distearoyl-*sn*-linoleoyl-glycerol, *J. Am. Oil Chem. Soc. 77*:1243–1249 (2000).
25. Lopez, C., P. Leieur, G. Keller, and M. Ollivon, Crystallization in Emulsion: Application to Thermal and Structural Behavior of Milk Fat, in *Crystallization and Solidification Properties of Lipids,* edited by N. Widlak, R.W. Hartel, and S.S. Narine, AOCS Press, Champaign, 2001, pp. 190–199.
26. Takeuchi, M., S. Ueno, E. Flöter, and K. Sato, Binary Phase Behavior of 1,3-Distearoyl-*sn*-oleoylglycerol (SOS) and 1,3-Distearoyl-*sn*-linoleoylglycerol (SLS), *J. Am. Oil Chem. Soc. 79*: 627–632.
27. Lopez, C., P. Leieur, G. Keller, and M. Ollivon, Thermal and Structural Behavior of Milk Fat: 1 Unstable Species of Cream, *J. Colloid Interface Sci. 229*:62–71 (2000).
28. Lopez, C., P. Leieur, C. Bourgaux, G. Keller, and M. Ollivon, Thermal and Structural Behavior of Milk Fat: 2 Crystalline Forms Obtained by Slow Cooling of Cream, *Ibid. 240*:150–161 (2001).
29. Lopez, C., A. Riaublanc, P. Leieur, C. Bourgaux, G. Keller, and M. Ollivon, Definition of a Model Fat for Crystallization-in-Emulsion Studies, *J. Am. Oil Chem. Soc. 78*:1233–1244 (2001).
30. Coupland, J., E. Dickinson, D.J. McClements, M. Povey, and C.R. Mimmerand, Crystallization in Simple Paraffins and Monoacid Saturated Triacylglycerols Dispersed in Water, in *Food Colloids and Polymers: Stability and Mechanical Properties*, edited by E. Dickinson and P. Walstra, The Royal Society of Chemistry, Cambridge, 1993, pp. 243–249.
31. Povey, M.J.W., Crystallization of Oil-in-Water Emulsions, in *Crystallization Processes in Fats and Lipid Systems,* edited by N. Garti and K. Sato, Marcel Dekker, New York, 2001, pp. 251–288.
32. Awad, T.S., Y. Hamada, and K. Sato, Effects of Addition of Diacylglycerols on Fat Crystallization in Oil-in-Water Emulsion, *Eur. J. Lipid Sci. Technol. 103*:734–741 (2001).
33. Katsuragi, T., N. Kaneko, and K. Sato, Effects of Addition of Hydrophobic Sucrose Fatty Acid Oligoesters on Crystallization Rates of *n*-Hexadecane in Oil-in-Water Emulsions, *Colloid Surf. B 20*:229–237 (2001).
34. Hamada, Y., I. Kobayashi, M. Nakajima, and K. Sato, Optical and Interfacial Tension Study of Crystallization of *n*-Alkane in Oil-in-Water Using Mono-dispersed Droplets, *Crystal Growth Design 2*:579–584 (2002).
35. Aquilano, D., and G. Squaldino, Fundamental Aspects of Equilibrium and Crystallization Kinetics, in *Crystallization Processes in Fats and Lipid Systems*, edited by N. Garti and K. Sato, Marcel Dekker, New York, 2001, pp. 1–51.
36. Flack, E., Butter, Margarine, Spread and Baking Fats, in *Lipid Technologies and Applications,* edited by F.D. Gunstone and F.B. Padley, Marcel Dekker, New York, 1997, pp. 305–327.

[Received June 10, 2002; accepted March 28, 2003]